

Electronic structure and optical properties of Ge-and F-doped α -Ga_2O_3: First-principles investigations

Ti-Kang Shu(束体康), Rui-Xia Miao(苗瑞霞)†, San-Dong Guo(郭三栋), Shao-Qing Wang(王少青), Chen-He Zhao(赵晨鹤), and Xue-Lan Zhang(张雪兰)

Citation: Chin. Phys. B, 2020, 29 (**12**): 126301. DOI: 10.1088/1674-1056/abbbff
Journal homepage: http://cpb.iphy.ac.cn; http://iopscience.iop.org/cpb

What follows is a list of articles you may be interested in

Surface-regulated triangular borophene as Dirac-like materials from density functional calculation investigation

Wenyu Fang(方文玉), Wenbin Kang(康文斌), Jun Zhao(赵军), Pengcheng Zhang(张鹏程)
Chin. Phys. B, 2020, 29 (**9**): 096301. DOI: 10.1088/1674-1056/ab9bff

First-principles study of structural, mechanical, and electronic properties of W alloying with Zr

Ning-Ning Zhang(张宁宁), Yu-Juan Zhang(张玉娟), Yu Yang(杨宇), Ping Zhang(张平), Chang-Chun Ge(葛昌纯)
Chin. Phys. B, 2019, 28 (**4**): 046301. DOI: 10.1088/1674-1056/28/4/046301

Superconductivity in electron-doped arsenene

Xin Kong(孔鑫), Miao Gao(高淼), Xun-Wang Yan(闫循旺), Zhong-Yi Lu(卢仲毅), Tao Xiang(向涛)
Chin. Phys. B, 2018, 27 (**4**): 046301. DOI: 10.1088/1674-1056/27/4/046301

Structural, electronic, and magnetic behaviors of 5d transition metal atom substituted divacancy graphene: A first-principles study

Rafique Muhammad, Yong Shuai(帅永), He-Ping Tan, Hassan Muhammad
Chin. Phys. B, 2017, 26 (**5**): 056301. DOI: 10.1088/1674-1056/26/5/056301

Mechanical and thermodynamical stability of $BiVO_4$ polymorphs using first-principles study

A K M Farid Ul Islam, Md Nurul Huda Liton, H M Tariqul Islam, Md Al Helal, Md Kamruzzaman
Chin. Phys. B, 2017, 26 (**3**): 036301. DOI: 10.1088/1674-1056/26/3/036301

Electronic structure and optical properties of Ge- and F-doped α-Ga_2O_3: First-principles investigations*

Ti-Kang Shu(束体康), Rui-Xia Miao(苗瑞霞)†, San-Dong Guo(郭三栋),
Shao-Qing Wang(王少青), Chen-He Zhao(赵晨鹤), and Xue-Lan Zhang(张雪兰)

School of Electronic Engineering, Xi'an University of Posts & Telecommunications, Xi'an 710121, *China*

(Received 1 August 2020; revised manuscript received 7 September 2020; accepted manuscript online 28 September 2020)

The prospect of α-Ga_2O_3in optical and electrical devices application is fascinating. In order to obtain better performance, Ge and F elements with similar electronegativity and atomic size are selected as dopants. Based on density functional theory (DFT), we systematically research the electronic structure and optical properties of doped α-Ga_2O_3 by GGA+U calculation method. The results show that Ge atoms and F atoms are effective n-type dopants. For Ge-doped α-Ga_2O_3, it is probably obtained under O-poor conditions. However, for F-doped α-Ga_2O_3, it is probably obtained under O-rich conditions. The doping system of F element is more stable due to the lower formation energy. In this investigation, it is found that two kinds of doping can reduce the α-Ga_2O_3 band gap and improve the conductivity. What is more, it is observed that the absorption edge after doping has a blue shift and causes certain absorption effect on the visible region. Through the whole scale of comparison, Ge doping is more suitable for the application of transmittance materials, yet F doping is more appropriate for the application of deep ultraviolet devices. We expect that our research can provide guidance and reference for preparation of α-Ga_2O_3 thin films and photoelectric devices.

Keywords: DFT, GGA+U calculation method, α-Ga_2O_3, doping

PACS: 63.20.dk, 73.20.At, 74.20.Pq, 78.20.Ci **DOI:** 10.1088/1674-1056/abbbff

1. Introduction

Wide band gap semiconductors tend to be fascinating because of its unique material properties and great potential in the future.[1–5] By virtue of wide band gap (4.9 eV–5.6 eV) and high electric breakdown field,[6–8] Ga_2O_3 has become an attractive material for a wide range of applications, including solar-blind ultraviolet (UV) photodetector,[9,10] gas sensor,[11,12] transparent conductive film.[13] In general, it has five phases (α, β, γ, ε, and δ), the investigations on β-Ga_2O_3 are most extensive in the past few years.[14–17] Recently, however, other phases receive attention.[18–22] α-Ga_2O_3 has emerged as an attracting material owing to wider bandgap (5.5 eV) and smaller electron effective mass compared with β-Ga_2O_3.[23–26]

Several successful methods for preparing α-Ga_2O_3 thin films have been reported, such as halide vapor phase epitaxy (HVPE),[27] mist chemical vapor deposition (MIST-CVD),[28] and laser molecular beam epitaxy (LMBE).[29] On this ground, it was applied to solar-blind photodetectors and Schottky barrier diodes (SBDs). For instance, the nanoplasmonically enhanced α-Ga_2O_3 solar-blind photodetectors with an interdigital structure were fabricated on sapphire.[30] It gained a significant increase in responsivity at the solar-blind region, and the response peak located at 244 nm reached 3.36 A/W under an applied voltage of 5 V. Besides, Kentaro *et al.*[31] reported α-Ga_2O_3 based SBDs power device and the lowest on-resistance is 0.1 m$\Omega\cdot$cm^2. Therefore, it is foreseeable that α-Ga_2O_3 has an exciting prospect in the fields of devices.

Despite numerous accounts of experimental studies on α-Ga_2O_3, its theoretical research is comparatively minor and gradually begins to receive attention in the late period. In 2019, Dong *et al.*[26] examined the influence of the doping of Si, Sn, and Mg elements in α-Ga_2O_3 by first-principles investigations. Besides, Takuma *et al.*[32] reported the energetics and the electronic structure of native point defects in α-Ga_2O_3. The low carrier concentration of intrinsic α-Ga_2O_3 hinders the further application of this material. Doping is a very efficient method to improve the electrical properties of materials. In order to obtain more ideal performance, it is necessary to research the influence of different elements systematically doping on α-Ga_2O_3 from the theory, which is of great significance for further exploration of high conductivity films and applications based on α-Ga_2O_3 electronic and optical devices.

In this investigation, Ge and F atoms have similar electronegativity and atomic radii as those of Ga and O atoms, respectively. Therefore, we systematically research the electronic structure and optical properties of Ge- and F-doped α-Ga_2O_3 by GGA+U calculation method, so as to provide a reference for further experiments.

*Project supported by the National Natural Science Foundation of China (Grant No. 51302215) and the Natural Science Basic Research Program of Shaanxi Province, China (Grant Nos. 2018JQ6084 and 2019JQ-860).

†Corresponding author. E-mail: miao9508301@xupt.edu.cn

© 2020 Chinese Physical Society and IOP Publishing Ltd

2. Model and methods

$\alpha-Ga_2O_3$ has the corundum crystal structure and space group is *R*-3*C*. Figure 1 describes the pure and doped α-Ga_2O_3 models and the optimized conventional model is displayed in Fig. 1(a). It has two independent lattice parameters *a* and *c*, a is equal to *b*. Oxygen ions are approximately hexagonal close-packed and the gallium ions occupy two-thirds of the octahedral sites. Each Ga octahedron shares one face and three edges with three other octahedra.[25] To analyze stability of the doping system and other properties, we construct a 2×2×1 supercell of α-Ga_2O_3as the parent model, which is displayed in Fig. 1(b). Ge and F atoms as potential n-type dopants are investigated to explore their substitution for Ga and O atoms, respectively.

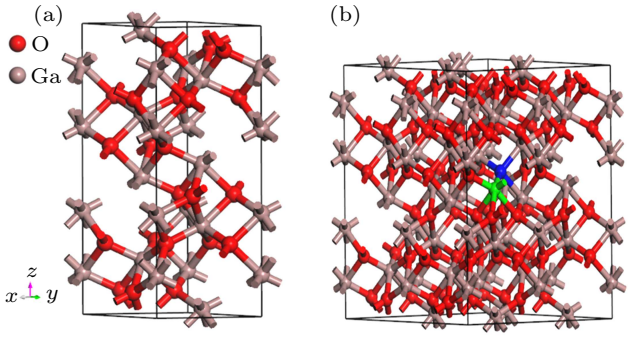


Fig. 1. (a) The optimized conventional structure, where gray represents Ga atoms and red signify O atoms and (b) the parent model of elements doped 2×2×1 supercell, among them, the green part represents Ga atom substituted doping, and the blue part represents O atom substituted doping.

All calculations were performed using the CASTEP code.[33] The exchange–correlation potential was described with the Perdew–Burke–Ernzerhof (PBE) functional in the Generalized Gradient Approximation (GGA),[34] and ultrasoft pseudo-potential was used for electron interactions. The valence electron configurations are Ga: [Ar] $3d^{10}4s^24p^1$, O: [He] $2s^22p^4$, Ge: [Ar] $3d^{10}4s^24p^2$, and F: [He] $2s^22p^5$. The GGA+*U* calculation methods were adopted to get an accurate band gap and theoretical results, where the *U* values of Ga-3d states and O-2p states were set to 14.0 eV and 8.35 eV,[16,35] respectively. We used 2×2×1 supercell of α-Ga_2O_3, the plane-wave basis energy cutoff was set to be 450 eV. A Monkhorst–Pack 6×3×2 *k*-point mesh was used in the whole reduced Brillouin zone.[36] The tolerance energy, maximum force, maximum stress, and maximum displacement were set to be 1×10^{-5} eV/atom, 0.03 eV/ Å, 0.05 GPa, and 0.001 Å, respectively.

3. Results and discussion

3.1. Crystal structure and analysis of stability

First, we investigate the pure α-Ga_2O_3. Table 1 lists the lattice constants of this calculation and the previous data. It can be found that these are consistent with the previous results.[25,26,37] Demonstrating that our model and calculation are reasonable.

Investigating the formation energy and transformation level is an effective method to judge the structural stability and rationality of Ge and F-doped Ga_2O_3. For the doping with a given charge state of *q*, the doping forming energy of the system is calculated according to the following formula:[16,26,32,38]

$$H^{\mathrm{f}}(\mathrm{doping},q) = E_{\mathrm{T}}(\mathrm{doping},q) - E_{\mathrm{T}}(\mathrm{perfect}) - \sum_i \Delta n_i u_i + q(E_{\mathrm{f}} + E_{\mathrm{VBM}}), \quad (1)$$

where $H^{\mathrm{f}}(\mathrm{doping},q)$ represents the total energy of Ge- and F-doped supercell. $E_{\mathrm{T}}(\mathrm{perfect})$ denotes the total energy of α-Ga_2O_3 supercell without doping. Δn_i is the number of atoms subtracted or added from the ideal supercell (positive if added, negative if removed). u_i is the atomic chemical potential, which needs to be considered under O-rich or O-poor extreme crystal growth conditions. E_{f} signifies the Fermi energy level, which is considered within the calculated range of valence band minimum ($E_{\mathrm{f}} = 0$ eV) and conduction band minimum ($E_{\mathrm{f}} = 5.57$ eV). E_{VBM} is the energy of valence band maximum value.

Table 1. The lattice parameters of α-Ga_2O_3 from theoretical and experimental results.

	Function	Lattice parameters	
		a/Å	*c*/Å
This work	GGA+*U*	5.07	13.66
Previous[26]	GGA	5.07	13.67
Previous[25]	B3LYP	5.04	13.56
Experiment[37]	–	4.98	13.43

First, we calculate Ge- and F-doped Ga and O sites respectively. Finding that the formation energy of Ge substituting Ga atom is −1.57 eV, while the value of Ge substituting O atom is 9.94 eV. Besides, the formation energy of F substituting Ga and O atom is −2.62 eV and −9.29 eV, respectively. Therefore, Ge atom is more inclined to occupy the Ga site, yet the F atom is more inclined to occupy the O site.

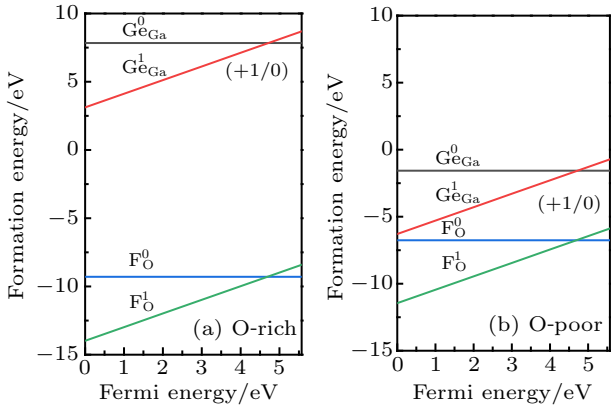


Fig. 2. The formation energies as a function of Fermi level for α-Ga_2O_3 with Ge and F substitution under (a) O-rich and (b) O-poor conditions.

According to Eq. (1), the doping formation energy of Ge-substituted Ga atom and F-substituted O atom is calculated respectively. What is more, we calculate the functional relationship of formation energy with Fermi energy level under the O-rich and O-poor growth conditions, which is plotted in Fig. 2. Under the O-rich condition, the formation energy of Ge doping is higher than that under the O-poor conditions. Therefore, Ge doping tends to be obtained under the O-poor conditions. For F doping, the formation energy of doping under the O-rich condition is lower than that under the O-poor condition. Thus, F doping is more likely to be obtained under the O-rich condition. In addition, the doping system of F element is more stable due to the lower formation energy. We also observed that the value of Ge_{Ga}^{+1} is lower than that of Ge_{Ga}^{0} in the range of 0 eV–4.72 eV, and increases with the Fermi energy level. On the contrary, the opposite phenomenon is observed in the range greater than 4.72 eV. Similar conclusions are obtained in F doping. The transition level $(+1/0)$ is at 0.85 eV and 0.88 eV below the conduction band minimum for Ge and F doped. In short, Ge and F atoms were found to be effective dopants by replacing Ga and O atoms, respectively.

3.2. Electronic structure

We first research the pure α-Ga_2O_3, as indicated in Fig. 3(a). It is found that the minimum value of the conduction band is at G (0,0,0), while the top of the valence band is only about 0.08 eV lower at G (0,0,0) than at F (0,1/2,0) k point. It results in a direct band gap of 5.65 eV at G and an indirect G–F band gap of 5.57 eV, compared with the experimental band gap (5.61 eV[39]) and the value (5.49 eV[32]) obtained by HSE calculation method, we consider the calculated results in this paper are reliable. Figures 3(c) and 3(e) show the band structure of the system after Ge and F elements doping, with band gaps of 5.434 eV and 5.438 eV, respectively. This indicates that the two dopings can reduce the band gap of the α-Ga_2O_3. In addition, neither of the two doping methods changed the properties of the indirect bandgap semiconductor of the α-Ga_2O_3.

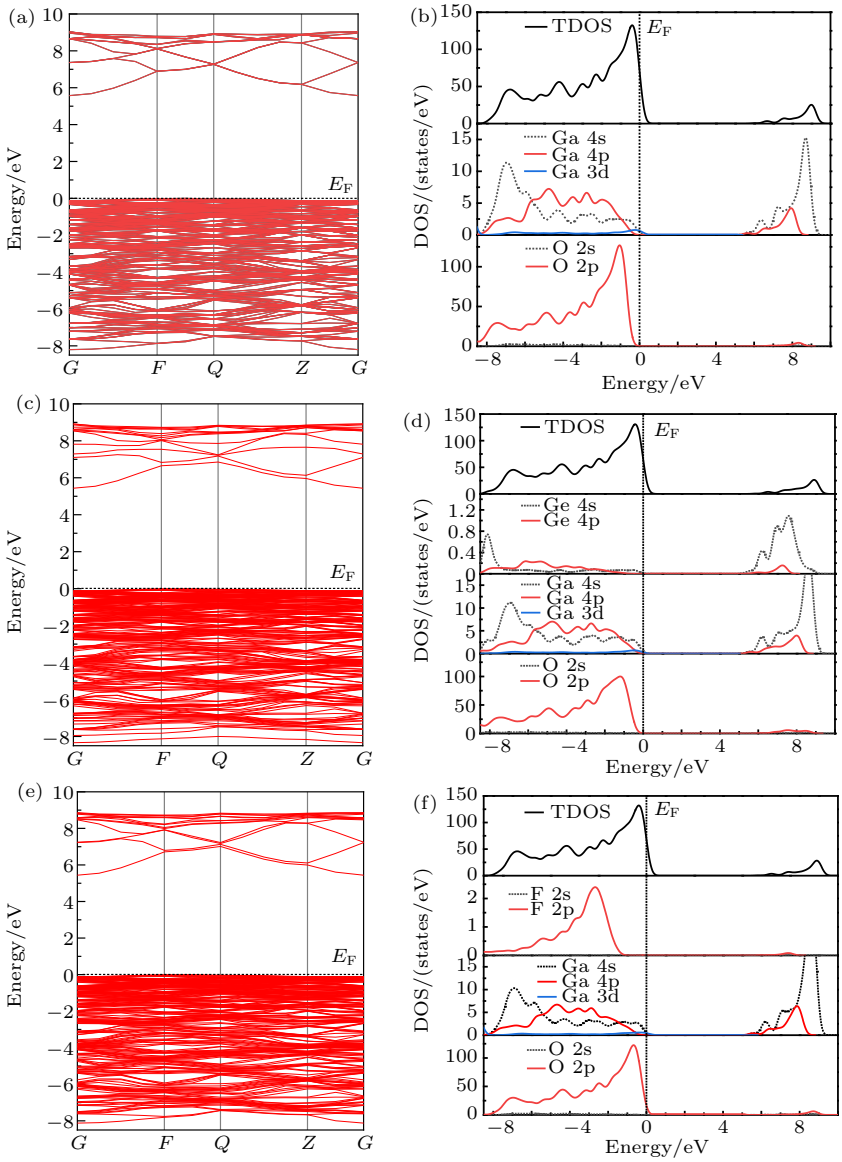


Fig. 3. The calculated band structure of (a) pure α-Ga_2O_3, (c) Ge-doped α-Ga_2O_3, and (e) F-doped α-Ga_2O_3; the calculated density of states of (b) pure α-Ga_2O_3, (d) Ge-doped α-Ga_2O_3, and (f) F-doped α-Ga_2O_3.

To better understand the electronic structure changes, figure 3(b) shows the density of states (DOS) of the pure α-Ga_2O_3. The upper valence band of the pure α-Ga_2O_3 is mainly occupied by the O-2p states which are likewise a common feature of oxide semiconductor materials. The conduction band is mainly contributed by Ga-4s and Ga-4p states, and Ga-4s states occupy the bottom of the conduction band. Thus, the band gap of α-Ga_2O_3 is mainly occupied by Ga-4s and O-2p states.

In an α-Ga_2O_3 supercell, when a Ga atom is substituted by a Ge atom, the density of states is depicted in Fig. 3(d). Doping does not alter the properties of the indirect bandgap semiconductor, but a large number of Ge-4s electrons appear in the conduction band. The Fermi level shifts slightly towards a high energy, with the band gap reduces to 5.434 eV. Besides, doping system displays n-type semiconductor characteristics. The reason for this is that after Ge^{4+} substitutes Ga^{3+}, an extra free electron is created. As a result, the electron concentration at the bottom of the conduction band increases and the Fermi level is pushed to a higher energy.[26,40] When an O atom is replaced by an F atom, as shown in Fig. 3(f), the F-2p contributes to the valence band, and the band gap reduces to 5.438 eV. It is also because after F^{1-} substitutes O^{2-}, more positive charges will be generated. In conclusion, we find that both Ge and F dopings are effective methods to let band structure achieve n-type α-Ga_2O_3. Meanwhile, the impurity level can also reduce the energy required to move carriers from the top of the valence band to the conduction band and improve the conductivity.

3.3. Optical properties

The dielectric function ($\varepsilon(\omega)$) is very significant for investigating the optical properties, which are almost related to the Kramers–Kronig dispersion. The real parts ($\varepsilon_1(\omega)$) and imaginary parts ($\varepsilon_2(\omega)$) of the dielectric function can be calculated by the following equations:[20,35]

$$\varepsilon(\omega) = \varepsilon_1(\omega)+\mathrm{i}\varepsilon_2(\omega), \tag{2}$$

$$\varepsilon(\omega) = 1+\frac{2}{\pi}\rho_0\int_0^{\infty}\frac{\omega'\varepsilon_2(\omega)}{\omega'^2-\omega^2}\mathrm{d}\omega, \tag{3}$$

$$\varepsilon_2(\omega) = \frac{C}{\omega^2}\sum_{V,C}\int_{BZ}\frac{2}{(2\pi)^3}|M_{CV}(k)|^2 \times\delta(E_C^k-E_V^k-\mathrm{h}\omega)\mathrm{d}^3k. \tag{4}$$

Among them, ρ_0 represents the density of medium, ω is the angular frequency, BZ is expressed as the first Brillouin zone. $|M_{CV}(k)|^2$ is indicated as the momentum transition matrix element. E_C^k and E_V^k denote the intrinsic energy levels, k is the inverted lattice.

As pictured in Fig. 4. In the pure α-Ga_2O_3, two distinct peaks can be found, the first peak at approximately 8.6 eV and the second smaller peak at roughly 16.1 eV. The former main peak is owing to the electron transition from the O-2p states to the Ga-4s states, the latter, smaller peak is generated by excitation of the Ga-3d electron to the Ga-4s conductive orbital. In the doping system of different substances, the position of the main peak doped by Ge element does not change much, while the main peak doped by F element moves to the low energy region. This may be related to the lattice distortion and impurity level formation caused by impurity incorporation.[41] Furthermore, the two kinds of doping produce small peaks with different strengths around 1.65 eV and 1.57 eV respectively. What is more, the strength of the peak doped by Ge element is greater than that of F element doping. For Ge doping, it is caused by the electron transition between Ge-4s states and O-2p states, for F element, occurs from the F-2p states and Ga-4s states. The strength difference between the two peaks may be ascribable to the fact that the Ge-4s states require only relatively low energy to achieve the electron transition compared to the F-2p states. These manifest that different dopants have different effects on the low energy region of α-Ga_2O_3. Moreover, the absorption edges move from 5.32 eV to 6.3 eV and 5.68 eV respectively, resulting in a blue shift. The above analyses indicate that the optical properties can be changed by changing the doping elements.

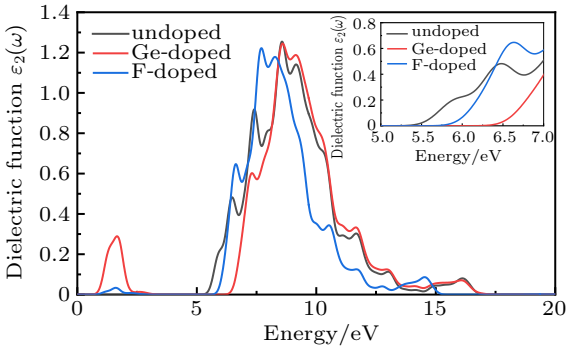


Fig. 4. The imaginary parts of the dielectric function.

The absorption coefficient ($\alpha(\omega)$) and reflectivity ($R(\omega)$) can be obtained by the following formula:[20,35]

$$\alpha(\omega) = \sqrt{2}\omega[\sqrt{\varepsilon_1^2(\omega)+\varepsilon_2^2(\omega)}-\varepsilon_1(\omega)]^{1/2}, \tag{5}$$

$$R(\omega) = \left|\frac{\sqrt{\varepsilon_1(\omega)+\mathrm{j}\varepsilon_2(\omega)}-1}{\sqrt{\varepsilon_1(\omega)+\mathrm{j}\varepsilon_2(\omega)}+1}\right|^2. \tag{6}$$

As seen in Fig. 5, the pure α-Ga_2O_3 has a great absorption effect on the light with a wavelength less than 223 nm, so it holds the potential of deep ultraviolet detection. Besides, in the visible light region, O-2p states and Ga-4s states are difficult to achieve electronic transition. When Ge and F elements are doped with α-Ga_2O_3, the light absorption moves from 223 nm to 197 nm and 218 nm, causing a blue shift. The cause may be that doping increases the energy required for electrons at the top of the valence band to transition to the conduction band, so high-energy light excites electrons and the absorption edges move towards violet light. Furthermore,

we observed that in the ultraviolet region, the absorption spectral strength of F element-doped is greater than that of the pure α-Ga_2O_3 and Ge element doped. However, in the visible region, Ge element doped absorption spectrum is stronger than the pure α-Ga_2O_3 and F element doped. The reason for this may be that, in the F-doped structure, electrons from the valence band need more energy to enter the conduction band, thus slowing the transition and decreasing absorption in the visible range. In a word, we find that a-Ga_2O_3 doped with two kinds of elements not only increased the absorption in the ultraviolet region, but also produced a certain absorption in the visible region, which provided a certain reference for the experiment.

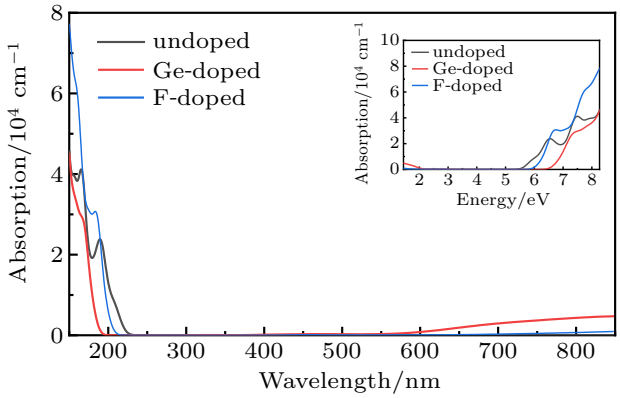


Fig. 5. The absorption coefficient of pure and doped α-Ga_2O_3.

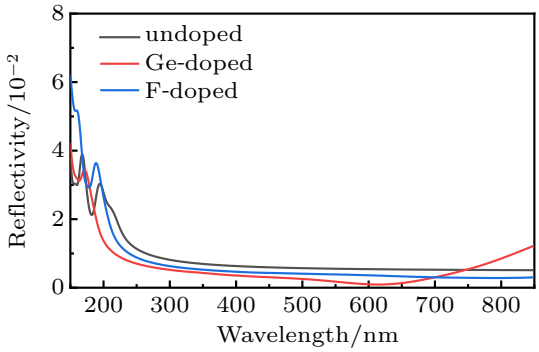


Fig. 6. The reflectivity of pure and doped α-Ga_2O_3.

It can be viewed from the reflectivity analysis in Fig. 6 that Ge- and F-doped α-Ga_2O_3 have high reflectivity in the ultraviolet region. For the visible light range, when the wavelength is less than 700 nm, the reflectivity of Ge doping is less than F doping. Nevertheless, when the wavelength is more than 700 nm, the opposite result is obtained. Through the whole scale of comparison, the former has a better transmittance, so it is more suitable for the application of transmittance materials. The latter has a higher absorption rate in the deep ultraviolet region, so it is more appropriate for the application of deep ultraviolet devices.

4. Conclusion

To sum up, the electronic structure and optical properties of Ge- and F-doped α-Ga_2O_3 are systematically studied by GGA+U calculation method. The results of crystal structure and stability calculation show that the Ge atom is more inclined to occupy the Ga site, yet the F atom is more inclined to occupy the O site, both are effective dopant. For Ge doping, it is probably obtained under O-poor conditions, while for F doping, it is probably obtained under O-rich conditions. The doping system of F element is more stable due to the lower formation energy. By analyzing the electronic structure, we find that neither of the two doping methods change the properties of the indirect bandgap semiconductor of the α-Ga_2O_3. The band gap decreased from 5.57 eV to 5.434 eV and 5.438 eV respectively, and displays n-type semiconductor characteristics. It can be seen from the dielectric function, absorption spectrum, and reflectivity of Ge- and F-doped α-Ga_2O_3, the absorption edge is blue-shifted, in the meantime, the doped absorption spectrum not only has a strong absorption effect on the ultraviolet region, but also has a certain absorption effect on the visible region. Through the whole scale of comparison, Ge doping is more suitable for the application of transmittance materials, yet F doping is more appropriate for the application of deep ultraviolet devices.

References

[1] Kyrtsos A, Matsubara M and Bellotti E 2017 *Phys. Rev. B* **95** 245202
[2] Cui Z, Ke X Z, Li E L and Liu T 2016 *Mater. Design* **96** 409
[3] Zhu Z W, Zheng J Y, Wang L, Xiong B, Sun C Z, Hao Z B, Luo Y, Han Y J, Wang J and Li H T 2017 *Chin. Phys. Lett.* **34** 030303
[4] Zhang Y M, Wang J F, Cai D M, Ren G Q, Xu Y, Wang M Y, Hu X J and Xu K 2020 *Chin. Phys. B* **29** 026104
[5] Huang H L, Tang X Y, Guo H, Zhang Y M, Wang Y T and Zhang Y M 2019 *Chin. Phys. B* **28** 010701
[6] Pearton S J, Yang J C, Cary P H, Ren F, Kim J, Tadjer M J and Mastro M A 2018 *Appl. Phys. Rev.* **5** 011301
[7] Pearton S J, Ren F, Tadjer M and Kim J 2018 *J. Appl. Phys.* **124** 220901
[8] Galazka Z 2018 *Semicond. Sci. Technol.* **33** 113001
[9] Guo D Y, Wu Z P, An Y H, Guo X C, Chu X L, Sun C L, Li L H, Li P G and Tang W H 2014 *Appl. Phys. Lett.* **105** 023507
[10] Guo X C, Hao N H, Guo D Y, Wu Z P, An Y H, Chu X L, Li L H, Li P G, Lei M and Tang W H 2016 *J. Alloys Compd.* **660** 136
[11] Nakagomi S, Sai T and Kokubun Y 2013 *Sensors and Actuators B-Chemical* **187** 413
[12] Mazeina L, Perkins F K, Bermudez V M, Arnold S P and Prokes S M 2010 *Langmuir: the ACS Journal of Surfaces and Colloids* **26** 13722
[13] Mi W, Li Z, Luan C N, Xiao H D, Zhao C S and Ma J 2015 *Ceram. Int.* **41** 2572
[14] Zatsepin D A, Boukhvalov D W, Zatsepin A F, Kuznetsova Y A, Gogova D, Shur V Y and Esin A A 2018 *Superlattices and Microstructures* **120** 90
[15] Zacherle T, Schmidt P C and Martin M 2013 *Phys. Rev. B* **87** 235206
[16] Dong L P, Jia R X, Xin B, Peng B and Zhang Y M 2017 *Sci. Rep.* **7** 40160
[17] Huang H L, Tang X Y, Guo H, Zhang Y M, Wang Y T and Zhang Y M 2019 *Chin. Phys. B* **28** 010701
[18] Cora I, Mezzadri F, Boschi F, Bosi M, Caplovicova M, Calestani G, Dodony I, Pecz B and Fornari R 2017 *Crystengcomm* **19** 1509
[19] Pavesi M, Fabbri F, Boschi F, Piacentini G, Baraldi A, Bosi M, Gombia E, Parisini A and Fornari R 2018 *Mater. Chem. Phys.* **205** 502
[20] Fornari R, Pavesi M, Montedoro V, Klimm D, Mezzadri F, Cora I, Pecz B, Boschi F, Parisini A, Baraldi A, Ferrari C, Gombia E and Bosi M 2017 *Acta Materialia* **140** 411
[21] Guo S D and Du H M 2020 *Eur. Phys. J. B* **93** 7
[22] Oshima Y, Villora E G, Matsushita Y, Yamamoto S and Shimamura K 2015 *J. Appl. Phys.* **118** 085301

[23] Sun H D, Li K H, Castanedo C G T, Okur S, Tompa G S, Salagaj T, Lopati S, Genovese A and Li X H 2018 *Crystal Growth & Design* **18** 2370
[24] Furthmuller J and Bechstedt F 2016 *Phys. Rev. B* **93** 115204
[25] H.Y. He, R. Orlando, M.A. Blanco, R. Pandey, E. Amzallag, I. Baraille, M. Rerat 2006 *Phys. Rev. B* **74** 195123
[26] Dong L P, Yu J G, Zhang Y M and Jia R X 2019 *Comput. Mater. Sci.* **156** 273
[27] Oshima Y, Vllora E G and Shimamura K 2015 *Appl. Phys. Express* **8** 055501
[28] Chikoidze E, von Bardeleben H J, Akaiwa K, Shigematsu E, Kaneko K, Fujita S and Dumont Y 2016 *J. Appl. Phys.* **120** 025109
[29] Guo D Y, Zhao X L, Zhi Y S, Cui W, Huang Y Q, An Y H, Li P G, Wu Z P and Tang W H 2016 *Mater. Lett.* **164** 364
[30] Qiao G, Cai Q, Ma T C, Wang J, Chen X H, Xu Y, Shao Z G, Ye J D and Chen D J 2019 *Acs Appl. Mater. Interfaces* **11** 40283
[31] Kaneko K, Fujita S and Hitora T 2018 *Jpn. J. Appl. Phys.* **57** 02
[32] Kobayashi T, Gake T, Kumagai Y, Oba F and Matsushita Y 2019 *Appl. Phys. Express* **12** 091001
[33] Clark S J, Segall M D, Pickard C J, Hasnip P J, Probert M I, Refson K and Payne M C 2005 *Zeitschrift Fur Kristallographie Crystalline Materials* **220** 567
[34] Perdew J P, Burke K and Ernzerhof M 1996 *Phys. Rev. Lett.* **77** 3865
[35] Dang J N, Zheng S W, Chen L and Zheng T 2019 *Chin. Phys. B* **28** 016301
[36] Monkhorst H J and Pack J D 1976 *Phys. Rev. B* **13** 5188
[37] Marezio M and Remeika J 1967 *J. Chem. Phys.* **46** 1862
[38] Zheng T, Wang Q, Dang J N, He W, Wang L Y and Zheng S W 2020 *Comput. Mater. Sci.* **174** 109505
[39] Segura A, Artus L, Cusco R, Goldhahn R and Feneberg M 2017 *Phys. Rev. Mater.* **1** 024604
[40] Dai J F, Suo Z Q, Li Z P and Gao S S 2019 *Results in Physics* **15** 102649
[41] Zhang L L, Xia T, Liu G A, Lei B C, Zhao X C, Wang S X and Huang Y N 2019 *Acta Phys. Sin.* **68** 017401 (in Chinese)